HEAT TRANSFER MODEL FOR A FLUIDISED BED ICE SLURRY GENERATOR

P.PRONK, J.W.MEEWISSE, C.A.INFANTE FERREIRA

Laboratory of Refrigeration and Indoor Climate Technology, Delft University of Technology
Mekelweg 2, 2628 CD Delft, the Netherlands, Tel. +31-15-278 6669, Fax. +31-15-278 7204

ABSTRACT

Many experimental studies show that the presence of solid particles in fluidised beds enhances wall-to-bed heat transfer coefficients with respect to flows without particles. This enhancement is ascribed to thermal conduction by solid particles and to disturbances of the laminar sublayer by particles. In gas fluidised beds the first mechanism plays a dominant role and in liquid fluidised beds the second.

Previous experiments on fluidised beds as ice slurry generator have shown stable ice slurry production and promising heat transfer rates. In this paper Jamialahmadi's model for liquid / solid fluidised bed heat exchangers is selected as the most promising model to predict the heat transfer rates in ice slurry fluidised bed generators. Then the implementation of this model in a dynamic simulation model of the secondary system coupled with the ice slurry generator is discussed. Experimental set-up data are used to validate the model predictions. Finally the model is used to identify some design parameter effects on the performance of the ice slurry generator.

1. INTRODUCTION

The fluidised bed heat exchanger has shown promising heat transfer rates while producing ice slurry for secondary cooling purposes (Meewisse, 2001). Further optimisation is however still required, as well as a better understanding of the ice formation process in fluidised beds. This paper aims to develop a suitable model that can describe heat and mass transfer rates and can be used to optimise operating conditions.

In Figure 1 a schematic display of a fluidised bed ice generator is given. It consists of one or more vertical tubes installed in a shell. Inside the tubes a fluidised bed is located, consisting of particles of for example steel or glass. The upward flowing ice slurry fluidises the particles. At the shell-side a primary refrigerant is evaporated, for example ammonia or a hydrocarbon, which cools the walls of the fluidised bed tubes. The continuous impact of steel particles on the walls prevents the formation of an ice layer on the inside surface of the fluidised bed tubes. The fluidised particles also continuously disturb the heat exchanging boundary layer, increasing heat transfer rates. Furthermore, the particles themselves transport heat through the fluidised bed.

In this paper models describing heat and mass transfer processes in fluidised bed systems are discussed. Qualitatively a promising type of model is selected, of which a first quantitative analysis is made. Results of numerical simulations with this model are compared with experimental data, after which a first optimisation for important parameters is made.
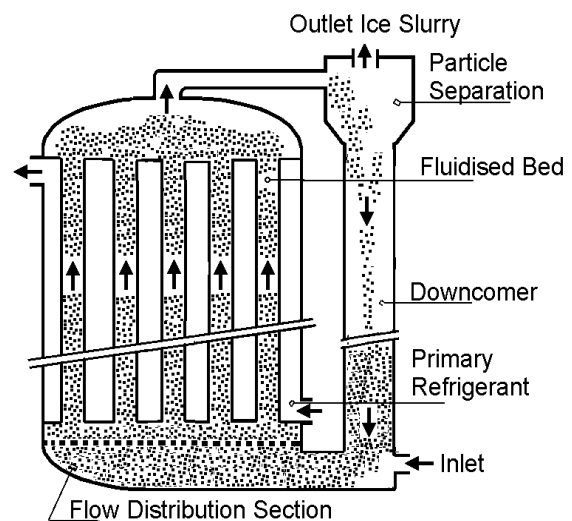

Figure 1 - Fluidised bed heat exchanger with particle circulation.

2. HEAT TRANSFER IN FLUIDISED BED HEAT EXCHANGERS

Experimental studies have shown that the presence of solid particles in fluidised beds can significantly enhance wall-to-bed heat transfer coefficients, compared to flows without particles (Haid et al., 1994). Three mechanisms improve wall-to-bed heat transfer in fluidised bed systems:

The first mechanism is based on conduction by solid particles during their contact with the heat-exchanging wall. Particles in the bulk of the fluidised bed have the same temperature as the fluid. Upon impact of particles on the wall, heat is transferred by conduction, altering the particle temperature. After the collision with the wall, the particles move back to the bulk of the fluidised bed, transferring the heat to the bulk fluid along the way.

The second mechanism is based on the disturbance of the laminar sublayer near the wall. Even if the flow in the bulk is turbulent, there is always a laminar sublayer near the heat exchanger wall representing the main thermal resistance of the heat transfer process. Collisions of solid particles at the wall disturb this sublayer, decreasing the thermal resistance and increasing heat transfer.

In gas-solid fluidised beds the first mechanism is the most important while the second mechanism plays a minor role. Ziegler and Brazelton (1964) have shown that the mechanism of particle conduction contributes 80 to 95% of the total heat transfer in gas-solid fluidised beds. The thermal conductivity and the volumetric heat capacity are much higher for liquids than for gases and therefore the second mechanism of heat transfer is expected to be dominant in liquid-solid fluidised beds.

The third effect is that the particles of the fluidised beds keep heat exchanging surface free of dirt and fouling, and in case of ice generators, prevent build up of an ice layer. Solids on heat exchanging walls give additional thermal resistance and can decrease heat transfer rates drastically. A schematic figure of the effect of fluidised bed particles for ice slurry systems is displayed in Figure 2.
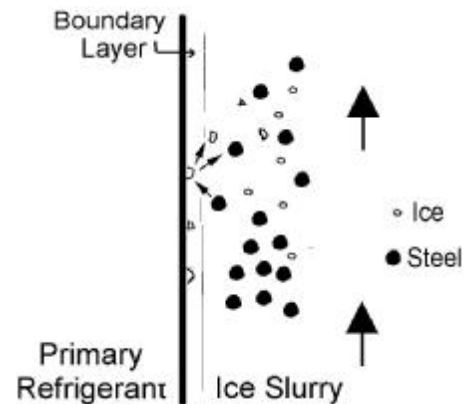

Figure 2 - Fluidised bed ice scraping effect

The fraction of the fluidised bed not occupied by particles, the bed porosity, has large influence on the heat transfer coefficient in liquid-solid fluidised beds. Heat transfer is at a maximum between bed porosity values of 0.6 and 0.8 (Haid et al, 1994, Jamialahmadi et al., 1997). This maximum is explained as follows: a higher bed porosity is caused by an enlargement of liquid velocity, which increases the motion of the particles. This increased particle motion creates more disturbances of the laminar layer and therefore enhances the heat transfer coefficient. On the other hand, a higher bed porosity also decreases the number of collisions on the wall and therefore decreases heat transfer. Both opposing effects result in a maximum of the heat transfer coefficient at a certain bed porosity. An example is given in Figure 3.
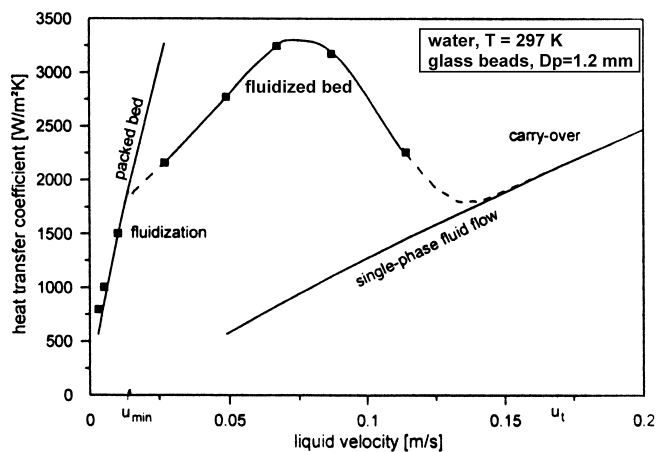

Figure 3 - Effect of liquid-solid fluidised bed on heat transfer coefficient (Haid et al., 1994)

3. SELECTION OF A HEAT TRANSFER MODEL

Two promising types of model were selected from literature for the prediction of wall-to-bed heat transfer rates in fluidised beds, one empirical and one theoretical. Both models have not earlier been tested for cooling or ice slurry production, but were derived for heating of process fluids.

Haid's model (empirical approach)
A lot of empirical studies describing heat transfer in fluidised beds can be found in literature. Haid et al. (1994) collected many empirical studies and summarised them. In all studies experiments were done with fluidised beds in which heat was transferred from the wall to the bed. In most water was used as the fluidisation liquid, only in a few cases tests were done with other liquids, such as oil or aqueous glycerine. Haid found that most of the expressions representing experimental data are of the form:

$$\mathrm{Nu}_p = C \cdot \mathrm{Re}_p^a \cdot \mathrm{Pr}^b \cdot \left(\frac{\rho_p - \rho_{liq}}{\rho_{liq}} \right)^c \cdot \left(\frac{D_p}{D_{bed}} \right)^d \cdot \varepsilon^e \cdot \left(1 - \varepsilon \right)^f \tag{1}$$

The model of Ruckenstein and Shorr, reported in previous work (Meewisse, 2000), also fits this general equation. To formulate a general empirical correlation, Haid collected test data from different experiments and combined these to quantify general values for the constant C and the exponents a to f in the correlation above. The following values were reported:

$$C = 0.1493 \ , \ a = 0.72 \ , \ b = 0.52 \ , \ c = 0.03 \ , \ d = 0.17 \ , \ e = -1.41 \ , \ f = 0.19 \tag{2}$$

Haid's model predicts the used measurement data with an average relative error of 32.8% and a standard deviation of 12.0%.

Jamialahmadi's model (theoretical approach)
Many theoretical models include only one of the processes mentioned in Section 2. However, one theoretical model for liquid-solid fluidised beds developed by Jamialahmadi et al. (1995 and 1996) includes both particle unsteady-state conduction and disturbance of the laminar boundary layer. The approach of this model is in analogy to nucleate boiling heat transfer models, whereby bubbles are replaced by particles. In the model the heat transfer surface is divided into two zones, one with particle effect and one without (See Figure 4). Heat transfer takes place simultaneously in both areas and heat transfer coefficients are calculated separately for the two different mechanisms.
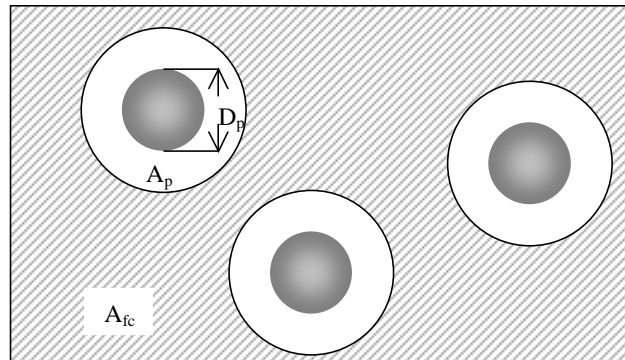

Figure 4 - Areas of heat exchanging walls of the model by Jamialahmadi

In the forced convection zone, the heat transfer coefficient α_{fc} can be calculated with well-known heat transfer expressions for single-phase turbulent flow, for example Gnielinski:

$$\alpha_{fc} = \frac{\lambda_{liq}}{D_{bed}} \cdot \frac{\frac{\xi}{8} \cdot (Re_{bed} - 1000) \cdot Pr}{1 + 12.7 \cdot \sqrt{\frac{\xi}{8}} \cdot (Pr^{2/3} - 1)} \cdot \left(1 + \left(\frac{D_{bed}}{L}\right)^{2/3}\right) \cdot \left(\frac{\mu}{\mu_w}\right)^{0.14}$$

(3)

$$\text{with } \xi = \left(1.82 \cdot^{10} \log(Re_{bed}) - 1.64\right)^{-2}$$

In the second zone, A_p, heat is transferred by unsteady-state conduction from the wall to the particle and to the liquid in the direct environment of the particle. The latter effect is in analogy with nucleate boiling where bubbles pump away the liquid from the wall. The analogy with particles leads to the assumption that a single particle affects the same area as a single bubble with the same size. The average heat transfer coefficient at the surface A_p is called α_p and is given by:

$$\alpha_p = \left(\frac{2}{\sqrt{\pi}} \sqrt{\lambda_{liq} \cdot \rho_{liq} \cdot c_{p,liq}} + K \cdot \sqrt{\lambda_p \cdot \rho_p \cdot c_{p,p}}\right) \cdot \frac{1}{\sqrt{\tau}}$$

(4)

The factor K in the expression is a constant that accounts for the area of contact between the particle and the wall, and is equal to 0.141 for cylindrical particles. The contact time t between the particle and the wall, is calculated by analogy to the kinetic theory of gases (Martin, 1981):

$$\tau = \frac{4}{3} \cdot \sqrt{\frac{D_p}{g} \cdot \left(\frac{\rho_p}{\rho_p - \rho_{liq}}\right) \cdot \left(\frac{5 \cdot (1 - \varepsilon_{PB}) \cdot (1 - \varepsilon)}{\varepsilon - \varepsilon_{PB}}\right)}$$

(5)

The total heat transfer coefficient can then be calculated with the following expression:

$$\alpha = \alpha_{fc} \cdot \frac{A_{fc}}{A} + \alpha_p \cdot \frac{A_p}{A}$$

(6)

The ratio A_p/A is determined by the number of particle impacts on the walls. It is assumed that a collision by a particle with a diameter of D_p influences an area of $\pi \cdot D_p^2$ on the wall. With this assumption the ratio A_p/A can be calculated as follows:

$$\frac{A_p}{A} = 1.5 \cdot \left(\frac{N_{BL}}{N}\right) \cdot \left(\frac{D_{bed}}{D_p}\right) \cdot (1 - \varepsilon)$$

(7)

The ratio N_{BL}/N represents the fraction of particles that is present in the boundary layer at a certain moment. Jamialahmadi determined this parameter empirically rather than theoretical, fitting the ratio to more than 3000 experimental data of liquid-solid fluidised beds found in literature. With this correlation, Jamialahmadi predicts the experimental data with an average relative error of 16.5%:

$$\frac{N_{BL}}{N} = 5.76 \cdot \left(\frac{D_p}{D_{bed}}\right)^{1.358} \cdot (\varepsilon - \varepsilon_{PB})^{0.353} \cdot (1 - \varepsilon)^{0.077}$$

(8)

Discussion on models
The operating conditions for the fluidised bed as ice slurry generator differ strongly from the experiments from which Haid fitted his expression. In the first place, most of those experiments

were performed for heating rather than for cooling purposes. Secondly, the properties of ice slurries are very different from aqueous solutions, especially the viscosity and the apparent heat capacity. The latter contains a sensible heat as well as a latent heat component, and can therefore be factors higher than the heat capacity of a liquid.

The different operating conditions were not included in the derivation of the theoretical model, because the fitted correlation in Jamialahmadi's model for the ratio N_{BL}/N only depends on mechanistic parameters, such as bed diameter, particle diameter and bed porosity. For this reason Jamialahmadi's model is mainly used in this work, but also results of Haid's model are studied.

4. EXPERIMENTAL SET-UP

At the Laboratory of Refrigeration and Indoor Climate Technology in Delft a fluidised bed heat exchanger was installed according to the schematic lay-out of Figure 5. The set-up consists of a single tube that can be operated in both stationary and circulating fluidised bed mode. The important parameters of the set-up are summarised in Table 1. During the experiments the downcomer tube was closed and the set-up was operated in the stationary mode.

Table 1 - Parameters of fluidised bed heat exchanger test set-up.

Heat exchanger			*Particles (cylindrical, stainless steel)*		
Internal diameter inner tube	56	mm	Average diameter	4	mm
Height	4.55	m	*Rotary positive displacement pump*		
Wall thickness	2	mm	Maximum flow rate	4	m³/h
Internal diameter outer tube	70	mm	*Primary refrigerant*		
Heat exchanging area	0.83	m²	Solution of potassium formiate	34	% wt.
Ice slurry			Flow rate	4	m³/h
Total system volume	130	l	Chiller capacity at −10 °C	5	kW
Freezing point depressant	NaCl				

In the set-up PT-100 sensors are used for temperature measurements. Two coriolis mass flow meters are used in the ice slurry circuit, which are also applied for density measurements from which ice content can be estimated. A pressure difference transmitter is installed inside the tube of the fluidised bed to detect the pressure drop over the fluidised bed.

The ice slurry pump is controlled either manually or automatically to keep either the flow rate or the pump input constant.

As primary refrigerant the set-up has been filled with an aqueous solution of potassium formiate, which flows counter-currently through the heat exchanger. The inlet temperature of the primary refrigerant can be controlled within 0.1 K with a control valve that bypasses part of the liquid flow.
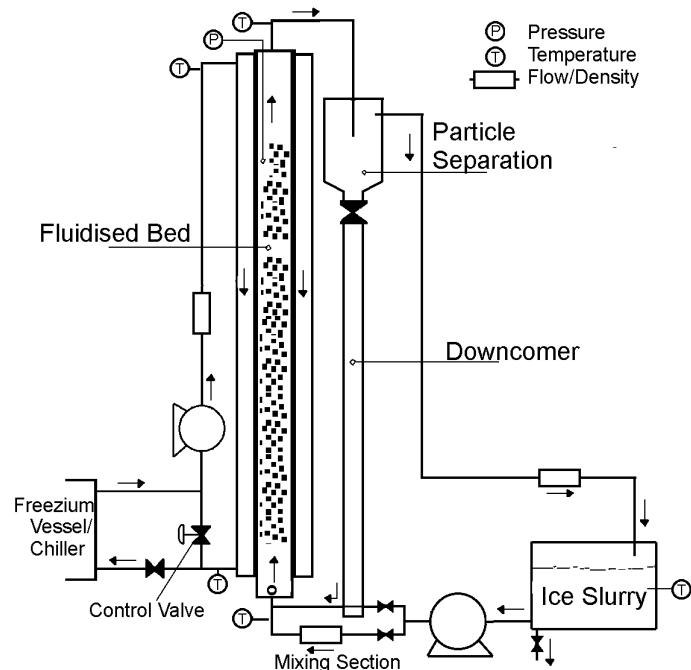
Figure 5 - Fluidised bed experimental set-up

5. SIMULATION OF THE FLUIDISED BED ICE SLURRY GENERATOR

A fluidised bed ice slurry generator with a single stationary fluidised bed was simulated using Jamialahmadi's model discussed in Section 3 and the dimensions of the experimental set-up described in Section 4.

The fluidised bed heat exchanger was simulated by dividing it into a finite number of cylindrical control volumes. In each control volume heat and mass balances on both the primary refrigerant side and the ice slurry side were solved by iteration with the Newton-Raphson method. The model started the simulation with the feed above the freezing point. After calculation of each control volume, it was checked whether the ice slurry feed had been cooled below its freezing point, after which the model was switched to the ice formation model. The temperature difference between the point just before ice formation starts and the freezing point of the solution, the supercooling, was hard to predict. Therefore 0.4 K was used as constant value for supercooling.

Apart from the fluidised bed the three following components were included in the simulation: Transport tubing, ice slurry storage vessel and pump. In the transport stage some heat losses occurred, and the tubing caused a significant part of the pressure drop over the entire system. This pressure drop together with the pressure drop of the fluidised bed was used to estimate the pumping power input. It was assumed that the power input of the pump was completely dissipated by melting of ice from the feed slurry. Since this phenomenon reduces the efficiency of the ice slurry system, the model can also be used to optimise for minimal pumping power input in future. In the storage vessel homogeneous ice slurry is assumed, because the return flow is being well mixed in the bulk of the storage vessel. Some heat losses were estimated for the storage vessel and also stirring power input could be taken into account.

After calculating all steps, calculations were summarised for the entire fluidised bed, for example heat flux, amount of ice produced, average overall heat transfer and the pressure drop over the entire fluidised bed, after which the simulation could be analysed.

Different kinds of freezing point depressants could be applied in the model by using data for secondary refrigerants reported by Melinder (1997). Also different types and sizes of particles could be selected as well as values for the heat exchanger parameters.

During the validation of the heat transfer models the heat exchanger was divided into eight control volumes and the time step was set at 0.5 seconds.

6. VALIDATION OF HEAT TRANSFER MODELS BY EXPERIMENTS

In order to validate the heat transfer models discussed in Section 3 experiments were carried out with the experimental set-up mentioned in Section 4. Table 2 gives an overview of the experiments:

Table 2 - Overview of experiments

No.	Concentr. NaCl	T freeze initial	T input prim. refr.	Bed porosity	Superficial velocity	Stable ice production	Super-cooling
	(%wt)	(°C)	(°C)	(-)	(m/s)	(-)	(K)
1	4.9	-3.0	-6.0	0.73	0.20	no	0.91
2	4.9	-3.0	-6.0	0.75	0.24	no	0.80
3	4.9	-3.0	-6.0	0.79	0.30	yes	0.58
4	4.9	-3.0	-6.0	0.83	0.36	yes	0.47
5	4.9	-3.0	-6.0	0.88	0.41	yes	0.38
6	7.9	-5.0	-8.0	0.79	0.30	yes	0.52
7	7.9	-5.0	-8.0	0.88	0.41	yes	0.47
8	10.6	-7.0	-10.0	0.79	0.30	yes	0.44
9	10.6	-7.0	-10.0	0.88	0.41	yes	0.39

Before the start of each experiment the experimental set-up was in equilibrium while the input temperature of the primary refrigerant was 3 K above the initial freezing temperature of the feed. At the start the input temperature of the primary refrigerant was lowered with 6 K at once, and the step response of the set-up was measured.

During the first part of each experiment the feed was cooled below its freezing temperature with a certain degree of supercooling, after which ice slurry was produced. In general the degree of supercooling was lower for a higher bed porosity and a higher concentration of freezing point depressant. Besides, it appeared that stable ice slurry production was not possible for a bed porosity lower than 0.79. In all other cases ice slurry production was stable and the experiment was continued until the ice slurry vessel contained at least 5% ice by weight.

After the experiments the results were compared with output from simulations in which Jamialahmadi's model was implemented. Most of these comparisons showed similar behaviour, and therefore one typical example is discussed here. Figures 6 and 7 show the behaviour of the temperature and the ice mass fraction at the outlet of the heat exchanger for both the experiment and the simulation for the conditions of experiment number 8.
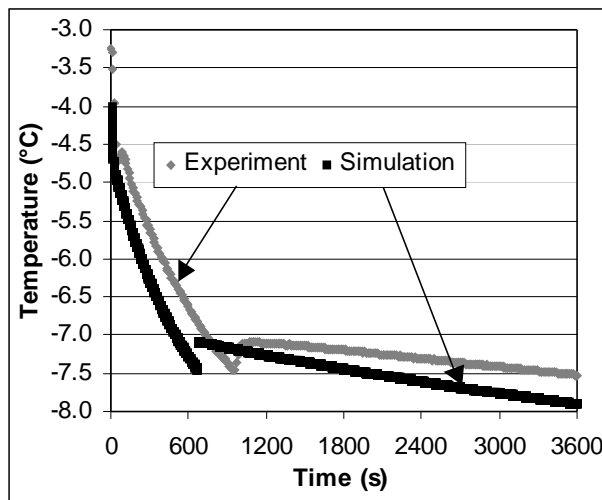

Figure 6 – Ice slurry temperature at the outlet of the heat exchanger
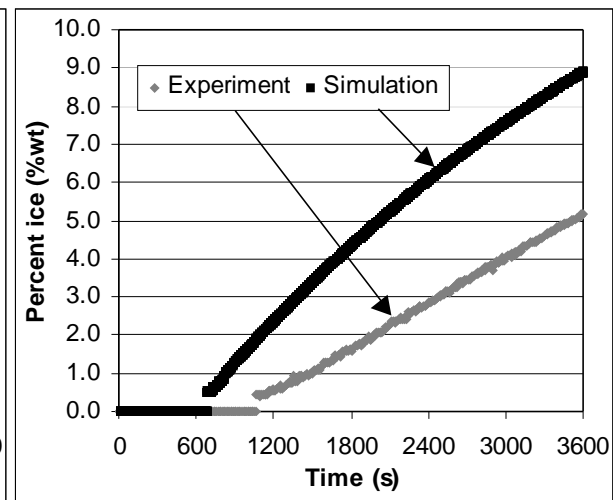

Figure 7 - Percent ice at the outlet of the heat exchanger

In general the simulations showed the same trend as the experiments, but the cooling process and the ice production in the simulations turned out to be much faster than in the experiments. The cause of this discrepancy was the difference in heat transfer coefficient as follows from Figure 8.

Jamialahmadi's model showed an enhancement in heat transfer coefficient after crystallisation had started mainly caused by the increase of apparent heat capacity. However,
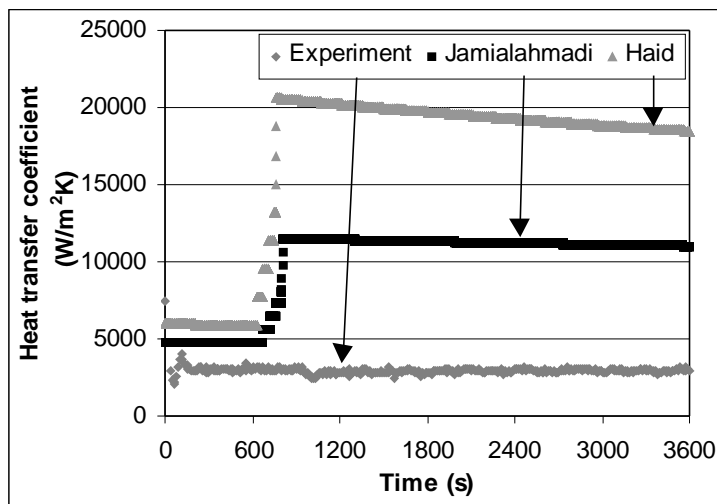

Figure 8 - Heat transfer coefficients at fluidised bed side

the heat transfer coefficient was quite constant during the experiment, with the remark that the value was slightly lower during crystallisation with respect to the value before crystallisation had started. Besides, the Jamialahmadi's model gave higher values for the heat transfer coefficient during the cooling phase with respect to the experimental values.

Some simulation results based on Haid's model are also shown in Figure 8. Haid's model showed the same trend as Jamialahmadi's model and overestimated heat transfer coefficient even more.

Similar to other fluidised bed heat exchangers the fluidised bed ice slurry generator showed a maximum in heat transfer coefficient at a certain bed porosity, which was about 0.79 based on Figure 9. Because stable ice slurry production was not possible at a bed porosity lower than 0.79, the heat transfer coefficients during the cooling phase were used to recognise this optimum. Figure 9 also shows convective heat transfer coefficients for a single-phase flow with the same velocity and heat capacity of the feed before crystallisation. From this can be deduced that the particles in the bed enhance the heat transfer coefficient by a factor of two to four with respect to a single-phase flow.
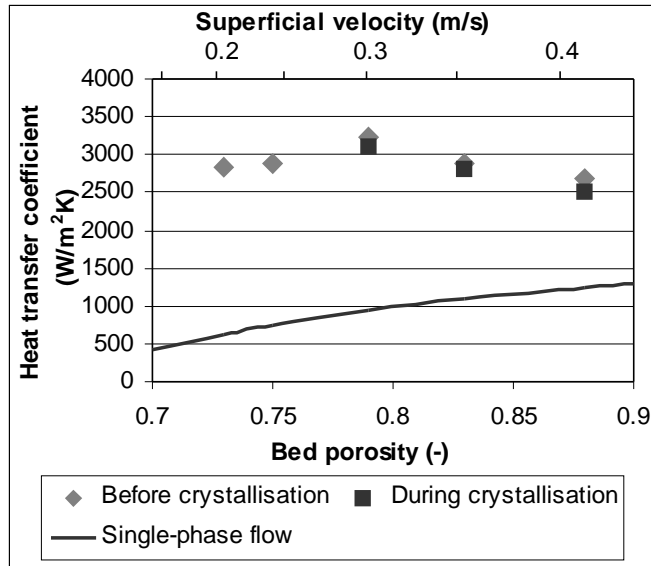

Figure 9 - Heat transfer coefficients at fluidised bed side for a solution of 4.9% NaCl

From the experiments was also concluded that higher concentrations of freezing point depressant generally cause lower heat transfer coefficients at the fluidised bed side. This phenomenon is ascribed to the fact that the higher liquid viscosity at higher concentrations and lower temperatures has a negative influence on the heat transfer process. In Figure 10 heat transfer coefficients at the fluidised bed side during crystallisation are shown as function of the concentration of NaCl at values for the bed porosity of 0.79 and 0.88. At a bed porosity of 0.88 the mentioned trend is more obvious than at a bed porosity of 0.79. More experiments are however needed to confirm this trend.
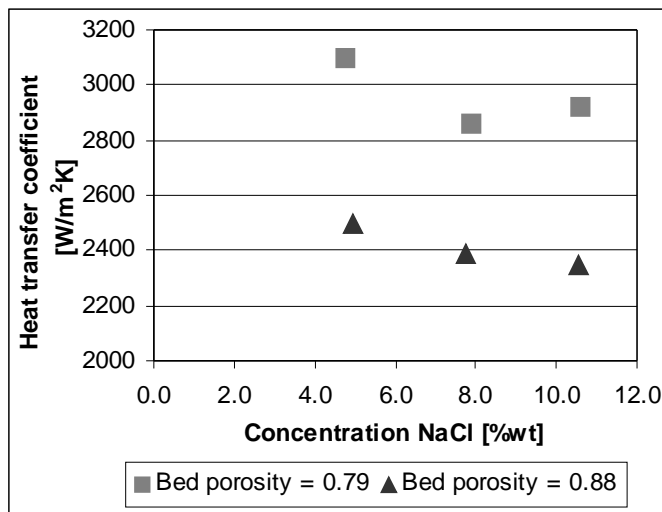

Figure 10 – Heat transfer coefficients at fluidised bed side at function of NaCl concentration

7. DISCUSSION

The comparison in Section 6 points out that in the experiments the crystallisation process only slightly changes the heat transfer coefficient. Both Jamialahmadi's model and Haid's model showed a significantly increase due to the increase in apparent heat capacity at the start of crystallisation. From this can be concluded that the latent component of the apparent heat capacity of ice slurry is not a very important factor in this ice slurry generator. A possible explanation is the fact that the heat transfer process near the wall is much faster than the crystallisation process whereby near the wall mainly sensible heat is transferred from the ice phase, the liquid phase, and the particles. As the ice slurry moves back from the wall the sensible heat is transformed into latent heat, increasing the ice fraction. Because the latent component of the apparent heat capacity does not seem to play an important role in this process, the heat capacity of ice slurry used in future heat transfer expressions should be represented as:

$$c_{p,is} = x \cdot c_{p,ice} + (1-x) \cdot c_{p,liq} \tag{9}$$

Furthermore can be concluded that both Jamialahmadi's model and Haid's model overestimate heat transfer coefficients during the cooling phase. Both models are therefore less suitable for the fluidised bed ice slurry generator.

Although Jamialahmadi's model is based on a theoretical approach, it appears that it is not suitable for all different kinds of liquid fluidised bed processes. It is possible that some of the assumptions in the model are not accurate, such as the area influenced by one particle or the contact time between the particle and the wall. Due to the fitted correlation (Equation 8) Jamialahmadi's model does show a good accuracy for the experiments where the mentioned correlation is based on, but gives poor results for fluidised beds with deviant operating conditions.

As stated above, Haid's model also gives poor results, which are also ascribed to deviant operating conditions. However, this model can be the baseline for a new correlation that is valid in the region of ice slurry production. Exponents for the density ratio and the diameter ratio in Equation 1 can be maintained, whereby experiments with other fluidised bed diameters and other kinds of particles are not necessary. Bremford et al. (2000) already showed that this method gives good results within a certain range of operating parameters.

8. CONCLUSIONS

Both Jamialahmadi's model and Haid's model are implemented in a dynamic simulation of an experimental set-up in order to predict heat transfer coefficients in a fluidised bed ice slurry generator. A comparison between experiments and results from simulations pointed out that both models overestimate heat transfer coefficients and that crystallisation does not affect the heat transfer process significantly. A possible explanation for the latter phenomenon is that the crystallisation takes place in the bulk of the fluidised bed instead of near the wall. The mean sensible heat capacity of ice slurry defined in Equation 9 should therefore be used instead of the apparent heat capacity, which is discussed in Section 3.

Since no suitable heat transfer model is available in literature, a new empirical correlation needs to be fitted with experimental data. This new correlation can be based on Haid's model in which some exponents can be maintained, reducing the number of experiments needed. This new model can be implemented in the simulation after which optimisation of the process becomes possible.

Although the selected models overestimated heat transfer coefficients, measured values are still high with respect to other ice slurry generators. A maximum in heat transfer coefficient was seen at a bed porosity of 0.79 and was about 3100 W/m^{2}K. Finally it was find out that an increasing concentration of freezing point depressant resulted in a slightly decrease in heat transfer coefficient.

NOMENCLATURE

A	Heat transfer area (m^2)	x	Ice mass fraction in ice slurry
A_{fc}	Forced convection area (m^2)	α	Heat transfer coefficient ($W/m^2 \cdot K$)
A_p	Particle conduction area (m^2)	α_{fc}	Forced convection heat transfer coefficient ($W/m^2 \cdot K$)
$c_{p,ice}$	Ice heat capacity ($J/kg \cdot K$)		
$c_{p,is}$	Ice slurry heat capacity ($J/kg \cdot K$)	α_p	Particle conduction heat transfer coefficient ($W/m^2 \cdot K$)
$c_{p,liq}$	Liquid heat capacity ($J/kg \cdot K$)		
$c_{p,p}$	Heat capacity of particle ($J/kg \cdot K$)	ε	Bed porosity
D_{bed}	Bed diameter (m)	ε_{PB}	Bed porosity packed bed
D_p	Particle diameter (m)	λ_p	Particle thermal conductivity ($W/m \cdot K$)
g	Acceleration due to gravity (m/s^2)	λ_{liq}	Liquid thermal conductivity ($W/m \cdot K$)
L	Fluidised bed length (m)	μ	Dynamic viscosity (Pa·s)
N	Number of particles in fluidised bed	μ_w	Dynamic viscosity at wall temperature (Pa·s)
N_{BL}	Number of particles in boundary layer		
Nu_p	Particle Nusselt number, $\alpha \cdot D_p / \lambda_{liq}$	ρ_{liq}	Liquid density (kg/m^3)
Pr	Prandtl number, $c_{p,liq} \cdot \mu / \lambda_{liq}$	ρ_p	Particle density (kg/m^3)
Re_{bed}	Reynolds number, $\rho_{liq} \cdot u \cdot D_{bed} / \mu$	τ	Contact time (s)
Re_p	Particle Reynolds number, $\rho_{liq} \cdot u \cdot D_p / \mu$	ξ	Gnielinski factor
u	Superficial liquid velocity (m/s)		

ACKNOWLEDGEMENT

REFERENCES

1. Bremford, D.J., Müller-Steinhagen, H., Duffy G.G., 2000, Heat Transfer to Kraft Black Liquor in a Liquid-Solid Fluidized Bed, *Heat Transfer Engineering*: vol.21, pp.57-69.
2. Haid, M., Martin, H., Müller-Steinhagen, H., 1994, Heat Transfer to Liquid-Solid Fluidized Beds, *Chemical Engineering and Processing*: vol.33, pp.211-225.
3. Jamialahmadi, M., Malayeri, M.R., Müller-Steinhagen, H., 1995, Prediction of Heat Transfer to Liquid-Solid Fluidized Beds, *Canadian Journal of Chemical Engineering*: vol.73, pp.444-455.
4. Jamialahmadi, M., Malayeri, M.R., Müller-Steinhagen, H., 1996, A Unified Correlation for the Prediction of Heat Transfer Coefficients in Liquid/Solid Fluidized Bed Systems, *Transactions of the ASME*: vol.118: pp.952-959.
5. Jamialahmadi, M., Malayeri, M.R., Müller-Steinhagen, H., 1997, 'Prediction of Optimum Operating Conditions of Liquid Fluidized Bed Systems, *Canadian Journal of Chemical Engineering*: vol.75, pp.327-332.
6. Martin, H., 1981, Fluid-bed heat exchanger – A New Model for Particle Convective Energy Transfer, *Chemical Engineering Communications*: vol.13, pp.1-16.
7. Meewisse, J.W., Infante Ferreira, C.A., 2000, Ice Slurry Production with a Fluidised Bed Heat Exchanger, *Second IIR Workshop on Ice Slurries*, *Paris, IIF/IIR*: pp.101-107.
8. Meewisse, J.W., Infante Ferreira, C.A., 2001, Experiments on Fluidised Bed Ice Slurry Production, *Third IIR Workshop on Ice Slurries, Lucerne, IIF/IIR*: pp.105-112.
9. Melinder, Á, 1997, *Thermophysical Properties of Liquid Secondary Refrigerants. Charts and Tables*', Handbook No.12 of the Swedish Society of Refrigeration.
10. Ziegler, E.N., Brazelton, W.T., 1964, Mechanisms of Heat Transfer to a Fixed Surface in a Fluidized Bed, *Industrial Engineering Chemical Fundamentals*: vol.3, pp.94-98.